Original papers
Materials for energy and environment, next-generation photovoltaics, and green technologies

УДК 544.723.212 DOI: 10.17277/jamt-2025-10-03-215-227

Kinetics of the lead ion sorption from aqueous solutions using underoxidized and overoxidized graphene oxides

© Ilya V. Tulupov[a], Lyubov E. Sosnovskikh[a], Viktoriya R. Ibragimova[b,c], Yuliya V. Ioni[b], Aleksei Yu. Isaev[a], Evgeny V. Galunin[a], Farid K. Shabiev[a,d], Gulnara N. Shigabaeva[a]✉

[a] *University of Tyumen, 6, Volodarskogo St., Tyumen, 625003, Russian Federation,*
[b] *Kurnakov Institute of General and Inorganic Chemistry of the Russian Academy of Sciences, 31, Leninskii Av., Moscow, 119991, Russian Federation,*
[c] *Lomonosov Moscow State University, 1, Leninskie Gory, Moscow, 119991, Russian Federation,*
[d] *Industrial University of Tyumen, 38, Volodarskogo St., Tyumen, 625000, Russian Federation*

✉ g.n.shigabaeva@utmn.ru

Abstract: The paper considers the kinetics of lead ions (Pb^{2+}) sorption from model aqueous solutions using underoxidized and overoxidized graphene oxide samples obtained from synthetic and natural (taken as comparison material) graphite. It was experimentally found that the contaminant is sorbed in the first 5 min (for the underoxidized samples) and 30 min (for the overoxidized samples), achieving a sorption capacity of 105–138 mg g^{-1}. Moreover, the capacity of the material increases with an increase in its oxidation state. The capacity of the synthetic material is slightly higher than that of the natural one. To study the removal mechanisms and determine the process parameters, the experimental data were fitted to kinetic (pseudo-first and pseudo-second order, as well as Elovich) and diffusion (internal diffusion – Morris-Weber and external diffusion – Boyd) models. It was found that the metal sorption is controlled by mixed diffusion of the sorbate into the bulk of the sorbent. It was also determined that this process is limited by the chemical interaction between the sorbent and the sorbate and depends on the sorbate concentration and the ambient temperature. Besides, the surface morphology of the samples was studied using scanning electron microscopy, and information on their elemental composition before and after the sorption was obtained using energy dispersive spectrometry, which confirmed the mechanism of the sorption processes occurring in the systems.

Keywords: graphene oxide; lead; sorption; sorption kinetics; nanomaterials; wastewater.

For citation: Tulupov IV, Sosnovskikh LE, Ibragimova VR, Ioni YuV, Isaev AYu, Galunin EV, Shabiev FK, Shigabaeva GN. Kinetics of the lead ion sorption from aqueous solutions using underoxidized and overoxidized graphene oxides. *Journal of Advanced Materials and Technologies*. 2025;10(3):215-227. DOI: 10.17277/jamt-2025-10-03-215-227

Кинетика сорбции ионов свинца из водных растворов с использованием недоокисленных и переокисленных оксидов графена

© И. В. Тулупов [a], Л. Е. Сосновских [a], В. Р. Ибрагимова [b,c], Ю. В. Иони [b], А. Ю. Исаев [a], Е. В. Галунин [a], Ф. К. Шабиев [a,d], Г. Н. Шигабаева [a]✉

[a] *Тюменский государственный университет, ул. Володарского, 6, Тюмень, 625003, Российская Федерация,*
[b] *Институт общей и неорганической химии им. Н. С. Курнакова РАН, Ленинский пр., 31, Москва, 119991, Российская Федерация,*
[c] *Московский государственный университет имени М. В. Ломоносова, Ленинские горы, 1, Москва, 119991, Российская Федерация,*
[d] *Тюменский индустриальный университет, ул. Володарского, 38, Тюмень, 625000, Российская Федерация*

✉ g.n.shigabaeva@utmn.ru

Аннотация: Рассмотрена кинетика сорбции ионов свинца (Pb^{2+}) из модельных водных растворов с использованием недоокисленных и переокисленных образцов оксида графена, полученных из синтетического и взятого в качестве сравнения натурального графита. Экспериментальным путем обнаружено, что поллютант

сорбируется в первые 5 (для переокисленных образцов) и 30 мин (для недоокисленных образцов), с достижением сорбционной емкости, равной 105…138 мг/г. Причем, емкость материала увеличивается с увеличением его степени окисления. У синтетического материала эта емкость немного выше, чем у натурального. Для изучения механизмов удаления и определения параметров процесса экспериментальные данные были сопоставлены с кинетическими (псевдо-первого и псевдо-второго порядка, а также Еловича) и диффузионными (внутренней диффузии – Морриса-Вебера и внешней диффузии – Бойда) моделями. Было установлено, что процесс сорбции металлов контролируется смешанной диффузией сорбата в основную массу сорбента. Также было определено, что данный процесс лимитируется химическим взаимодействием между сорбентом и сорбатом и зависит от концентрации сорбата и окружающей температуры. Кроме того, методом сканирующей электронной микроскопии была исследована морфология поверхности образцов и методом энергодисперсионной спектрометрии были получены сведения об их элементном составе до и после сорбции, которые подтверждают механизмы протекающих сорбционных процессов в системах.

Ключевые слова: оксид графена; свинец; сорбция; кинетика сорбции; наноматериалы; сточные воды.

Для цитирования: Tulupov IV, Sosnovskikh LE, Ibragimova VR, Ioni YuV, Isaev AYu, Galunin EV, Shabiev FK, Shigabaeva GN. Kinetics of the lead ion sorption from aqueous solutions using underoxidized and overoxidized graphene oxides. *Journal of Advanced Materials and Technologies*. 2025;10(3):215-227. DOI: 10.17277/jamt-2025-10-03-215-227

1. Introduction

Heavy metals are some of the primary pollutants found in wastewater. For example, in the Tyumen region, the most common metals found in wastewater are lead, nickel, cobalt, manganese, copper, cadmium, lead, and chromium [1]. As for lead, its main sources in such waters are enterprises engaged in galvanic and metallurgical production, as well as the production of inorganic fertilizers and pesticides [2]. Even low concentrations of this element in aquatic environments have a negative impact on the environment, human and animal health, causing dangerous diseases. Furthermore, the accumulation of lead in the soil can adversely impact the health of ecosystems [3]. Consequently, the removal of lead ions from wastewater has become a critical challenge in contemporary environmental science.

One of the methods for purifying wastewater from heavy metals is (ad)sorption – a process in which the (ad)sorbate (pollutant) settles on the surface of the (ad)sorbent. Activated carbons [4–6], cryogels [7–9], silica gels [10–12], nanoparticles [13], nanomaterials [14–16], bentonite clay [17, 18], and others are used as sorbents.

Recent scientific studies [19] addressing the topic of highly efficient water purification systems prove that carbon nanostructured materials have a higher sorption capacity compared to those mentioned above. Among such materials, graphene oxide holds a special place – a compound consisting of hydrogen, carbon, and oxygen atoms in various ratios, obtained by oxidizing graphite with strong oxidizers [20].

In this regard, the aim of the present paper is to study the kinetics of Pb^{2+} ion sorption on graphene oxides with different degrees of oxidation from model aqueous solutions. Sorption kinetics allows us to determine how the parameters of the system change over time and when equilibrium is reached. The removal of Pb^{2+} was conducted using under-oxidized and over-oxidized graphene oxides, which were obtained from graphite by oxidation with potassium permanganate in varying amounts.

2. Materials and Methods

2.1. Materials and reagents

To study the sorption properties of nanomaterials, the following materials were used: under-oxidized graphene oxide obtained from synthetic graphite (1.0 mass equivalent of $KMnO_4$) [Syn-UO-GO-1.0]; under-oxidized graphene oxide obtained from synthetic graphite (2.0 equivalent weights of $KMnO_4$) [Syn-UO-GO-2.0]; over-oxidized graphene oxide obtained from synthetic graphite (4.5 equivalent weights of $KMnO_4$) [Syn-OO-GO-4.5]; over-oxidized graphene oxide obtained from natural graphite (4.5 equivalent weights of $KMnO_4$) [Nat-OO-GO-4.5]. A sample of graphene oxide obtained from natural graphite was taken for comparison. All materials were provided by the Federal State Budgetary Institution of Science "N.S. Kurnakov Institute of General and Inorganic Chemistry of the Russian Academy of Sciences" (Moscow, Russia).

The basis of these materials – graphene oxide – was obtained using a modified Hummers' method. This method involves dispersing graphite in concentrated sulfuric acid (H_2SO_4) followed by the addition of potassium permanganate ($KMnO_4$) as an oxidizing agent. The amount of potassium

permanganate added correlated with the expected degree of oxidation and was 1, 2, and 4.5 equivalent weights of $KMnO_4$ per 1 g of graphite. The washing of the product was performed using solutions of hydrogen peroxide, 1 M hydrochloric acid, and an excess of distilled water through centrifugation (10,000 rpm for 10 min). The resulting samples of graphene oxide were air-dried in Petri dishes until a constant weight was achieved.

To prepare a solution simulating wastewater contaminated with lead, $Pb(NO_3)_2$ (reagent grade) and distilled water were used.

2.2. Sorption studies

The dependence of the sorption capacity on the contact time of underoxidized and overoxidized graphene oxide samples was determined based on the results of kinetic studies of Pb^{2+} ion sorption in a limited volume. The experimental conditions (in the static mode – batch) were as follows: 0.01 g of sorbent, 30 mL of Pb^{2+} solution of the initial concentration $C_{in} = 100$ mg·L^{-1}, the pH of the solution was not controlled, its initial value was 6.5–7.0, the sorption time was 5, 10, 30, 60, 90, 120 and 240 min. The phases in the test tubes were contacted by shaking them on a Multi Bio RS-24 rotator (BioSan Ltd., Riga, Latvia). To separate the samples (solid phase) from the solution (liquid phase) after the experiments, Blue Ribbon filter paper (pore sizes 1–2.5 nm) was used. The concentrations of lead ions in the solution at time t (C_t) were determined using a flame atomization atomic absorption spectrophotometer (ContrAA 700, Analyic Jena GmbH., Jena, Germany).

Based on the concentration values obtained as a result of the experiment before and after the sorption process, the sorption capacity of each material Q_e^{exp} was determined – a value showing how much substance the sorbent can absorb per unit mass (mg·g^{-1}). This parameter was calculated as follows [22]:

$$Q_e^{exp} = \frac{(C_{in} - C_t)V}{m}, \quad (1)$$

where C_{in} is initial concentration of pollutant mg·L^{-1}, C_t is pollutant concentration at a given time t, mg·L^{-1}, V is volume of solution, mL, and m is sorbent weight, g.

The rate of Pb^{2+} sorption on underoxidized and overoxidized graphene oxide samples was analyzed using empirical pseudo-first and pseudo-second order models, Elovich, and Morris-Weber and Boyd diffusion equations [23–27] (Table S1) (Supplementary materials).

To affirm that the processes outlined in Table 1 are taking place within the system, it is essential for the correlation coefficient (R^2) to be greater than or equal to 0.9 [28].

2.3. Analytic methods

The material samples were characterized using scanning electron microscopy (SEM) and energy-dispersive spectrometry (EDS) to determine the morphological features of their surface and elemental composition before and after Pb^{2+} sorption.

Scanning electron microscope (SEM) images were taken using a Tescan MIRA3 LMU microscope (Brno, Czech Republic) at an accelerating voltage of 5 kV. To improve the quality of the images, the samples were pre-coated with gold. For visual comparison, all samples were photographed in a field of 100 × 100 and 200 × 200 μm.

In addition to morphology imaging, the EDS method was used to confirm lead sorption using elemental analysis. The analysis was performed using an Oxford Instruments Ultim Max 65 microscope attachment (Abington, UK). The spectra were processed using the built-in software, and spectra were deconvolved by the element of the metal coating (gold) to clarify the quantitative data on the composition. When using spectra deconvolution, the contribution of the gold peak to the overall result was eliminated. Accordingly, elemental data were obtained as if there was no gold deposition.

3. Results and Discussion

3.1. Surface morphology and elemental composition of sorbents

To verify the assumptions about the mechanism of Pb^{2+} ion sorption on graphene oxide samples, the morphology and elemental composition of their surface were studied using SEM and EDS, respectively.

The surface of the Syn-OO-GO-4.5 sample has peaks and valleys with characteristic fractal geometry (Fig. 1*a*). This structure is otherwise called “wrinkled graphene” and is characteristic of the surface of graphene oxide [29]. When graphical analysis of the fractal dimension of the SEM-image of a certain area of the surface of this material using the box counting algorithm [30] showed that the fractal dimension is $D = 2.6034$. Additionally, small (1–2 μm in diameter)

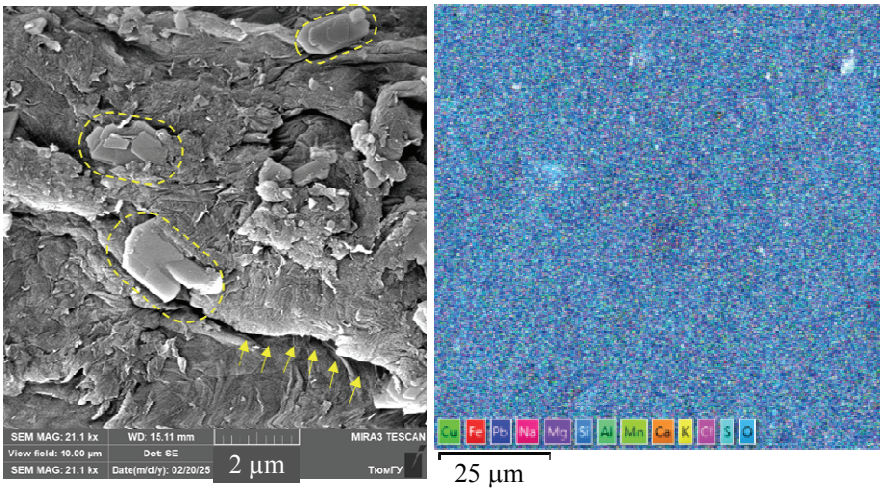

(a) *(b)*

Fig. 1. Carbon material Syn-OO-GO-4.5 before Pb^{2+} sorption:
a – SEM-image of the material surface (arrows indicate the wrinkle deepening);
b – multilayer EDS-image of the sample surface

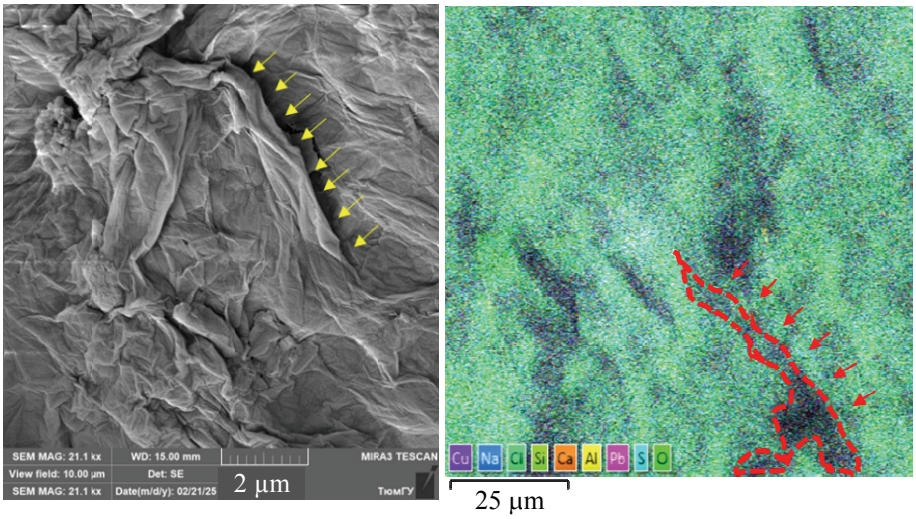

(a) *(b)*

Fig. 2. Carbon material Syn-OO-GO-4.5 after Pb^{2+} sorption:
a – SEM-image of the material surface (arrows indicate the fold deepening);
b – multilayer EDS-image of the sample surface

inclusions of graphite crystallites can be observed on the surface (highlighted by the yellow dotted line). In the multilayer EDS-image (Fig. 1*b*), a uniform distribution of various atoms (mainly oxygen and sulfur) can be observed. This is confirmed by the total spectrum after deconvolution – the content of oxygen atoms is 85.4 %, and sulfur is 10.1 % (Fig. S1) (Supplementary materials).

After sorption, the same material did not undergo any critical changes (Fig. 2*a*). Also, elevations and depressions are observed (shown by arrows in Fig. 2*a*), i.e., a "wrinkled" surface structure. Graphical analysis of the fractal dimension of the SEM-image of a certain area of the surface of this material after sorption shows that the fractal dimension has changed and became equal to $D = 2.5153$. A slight decrease in the fractal dimension can be associated with the coating of some of the elevations and depressions with pollutant (i.e., Pb^{2+}).

The multilayer EDS-image of the surface after Pb^{2+} sorption shows that lead atoms are distributed over the entire surface. However, in areas with wrinkles, mainly in the fold recesses, the concentration of lead atoms is higher (Fig. 2*b*, the area highlighted by the dashed-dotted line). The total combined weight of lead atoms is 34.7 % (Fig. S2).

The surface of the Nat-OO-GO-4.5 material has a surface morphology similar to that of the Syn-OO-

GO-4.5 material, i.e. peaks and valleys with characteristic fractal geometry can also be observed (Fig. 3*a*). The fractal dimension of the surface of this material is $D = 2.6181$. Similar to the Syn-OO-GO-4.5 material, small (0.5–1 μm in diameter) inclusions of graphite crystallites (highlighted by the yellow dotted line) can also be observed on the surface of the Nat-OO-GO-4.5 material. In the multilayer EDS-image (Fig. 3*b*), a uniform distribution of various atoms (mainly oxygen and sulfur) can be observed. The total weight of oxygen atoms is 83.3 %, sulfur – 10.9 % (Fig. S3).

After sorption, the Nat-OO-GO-4.5 material, similar to the previous material, did not change significantly (Fig. 4*a*). A wrinkled structure is also observed (shown by arrows in Fig. 4*a*). Just as on the surface of the Syn-OO-GO-4.5 material, inclusions in the form of graphite crystallites disappeared from the surface of the Nat-OO-GO-4.5 material. Graphic analysis of the fractal dimension of the sample under consideration after sorption shows that it changed and became equal to $D = 2.5291$, which is greater than for the surface of the Syn-OO-GO-4.5 material ($D = 2.5153$). The multilayer EDS-image (Fig. 4*b*) of the surface after Pb^{2+} sorption shows that lead atoms are distributed over the entire surface, but clusters are observed, indicated by arrows. Such clusters may be associated with a wrinkled structure. The total combined weight of lead atoms is 24.7 % (Fig. S4).

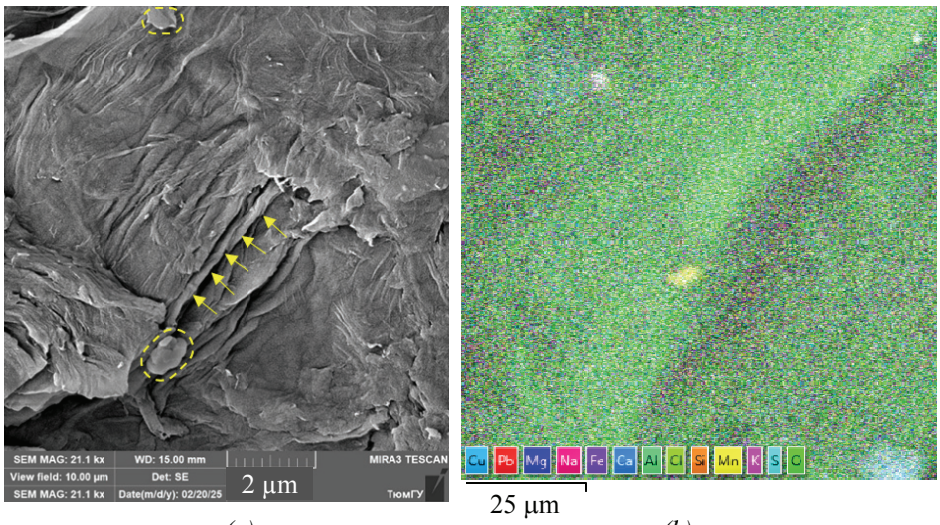

(a) *(b)*

Fig. 3. Carbon material Nat-OO-GO-4.5 before lead sorption:
a – SEM-image of the material surface (arrows indicate the fold deepening);
b – multilayer EDS-image of the sample surface

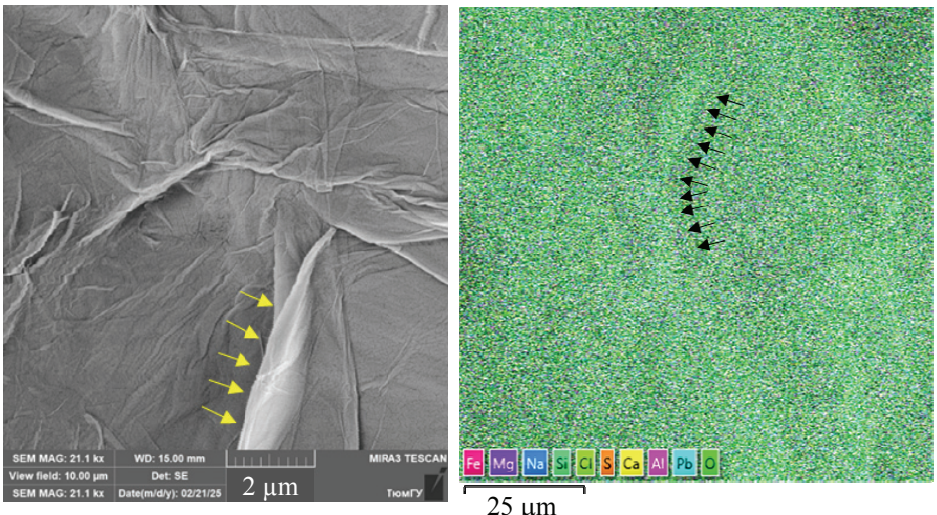

(a) *(b)*

Fig. 4. Carbon material Nat-OO-GO-4.5 after lead sorption:
a – SEM-image of the material surface (arrows indicate the elevation of the fold);
b – multilayer EDS-image of the sample surface (arrows indicate the lead concentration)

The surface of the Syn-UO-GO-1.0 material consists of individual particles of exfoliated graphite ~10 μm in size (Fig. 5*a*), the size of the exfoliations is about ~500 nm. Also, inclusions of clusters of spherical nanoparticles with a total diameter of ~2 μm can be observed on the surface. The fractal dimension is $D = 2.555$. In the multilayer EDS-image (Fig. 5*b*), a non-uniform distribution of various atoms (mainly oxygen and sulfur) can be observed. The total weight of oxygen atoms is 78.2 %, sulfur – 12.8 % (Fig. S5).

The surface of the Syn-UO-GO-1.0 material after sorption consists of individual particles of exfoliated graphite (Fig. 6*a*). On the surface, as before sorption, inclusions of clusters of spherical nanoparticles with a total diameter of 2–5 μm can be observed (areas highlighted by a dotted line). The fractal dimension changed insignificantly and amounted to $D = 2.5157$. In the multilayer EDS-image (Fig. 6*b*), a non-uniform distribution of lead atoms can be observed. The total weight of lead atoms is 15.4 % (Fig. S6).

The surface of the Syn-UO-GO-2.0 material before sorption consists of individual particles of exfoliated graphite, 10 μm in size (Fig. 7*a*). The exfoliations are about ~2 μm in size, which is 4 times greater than the exfoliations observed in the Syn-UO-GO-1.0 sample.

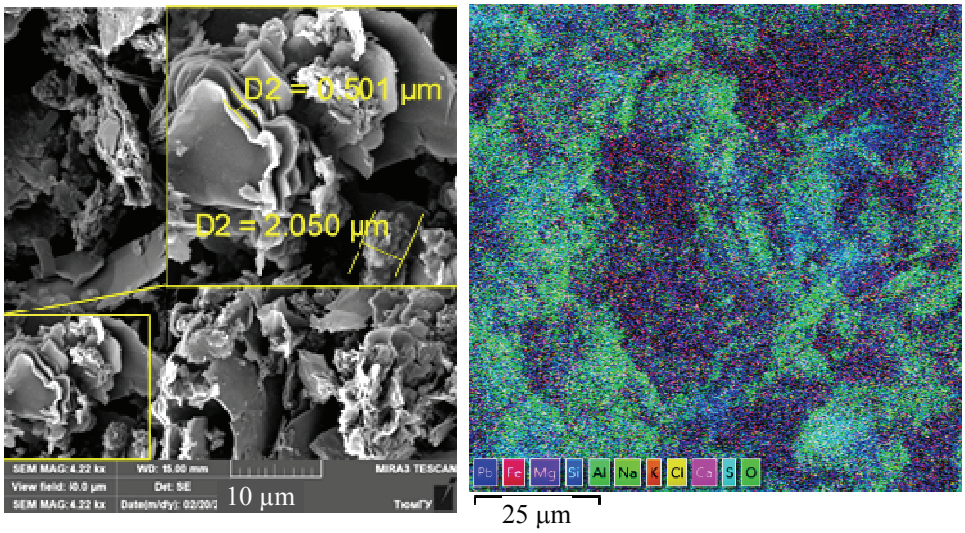

Fig. 5. Carbon material Syn-UO-GO-1.0 before lead sorption:
a – SEM-image of the material surface (the inset shows a section of exfoliated graphite);
b – multilayer EDS-image of the sample surface

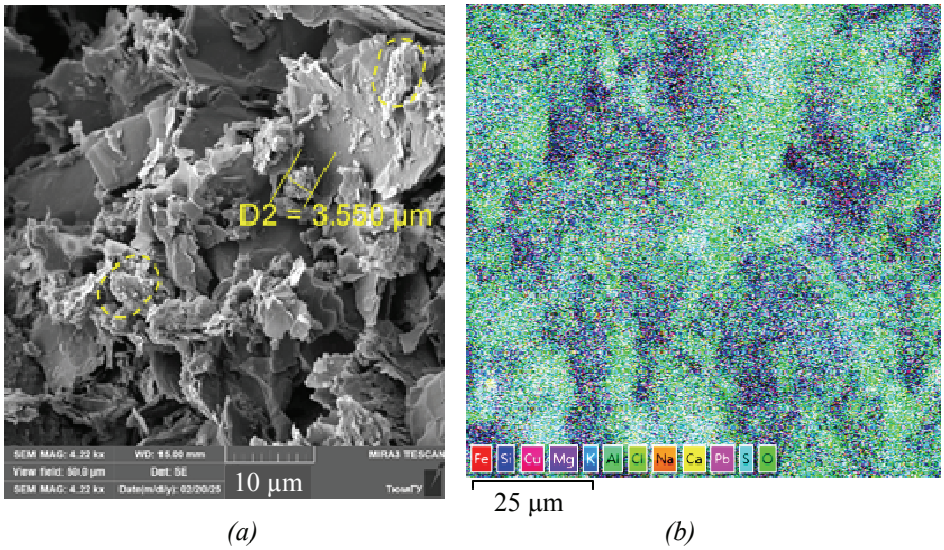

Fig. 6. Carbon material Syn-UO-GO-1.0 after lead sorption:
a – SEM-image of the material surface; *b* – multilayer EDS-image of the sample surface

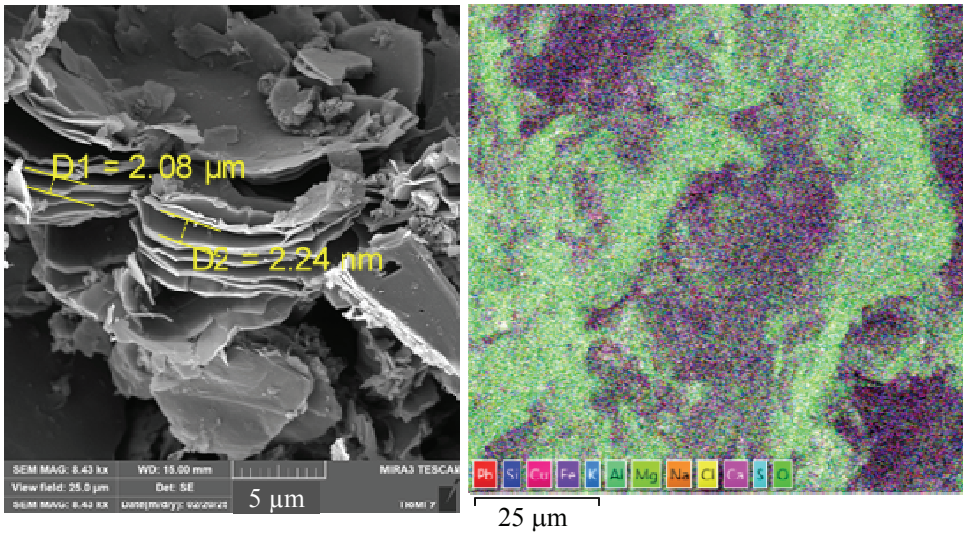

(a) *(b)*

Fig. 7. Carbon material Syn-UO-GO-2.0 before lead sorption:
a – SEM-image of the material surface; *b* – multilayer EDS-image of the sample surface

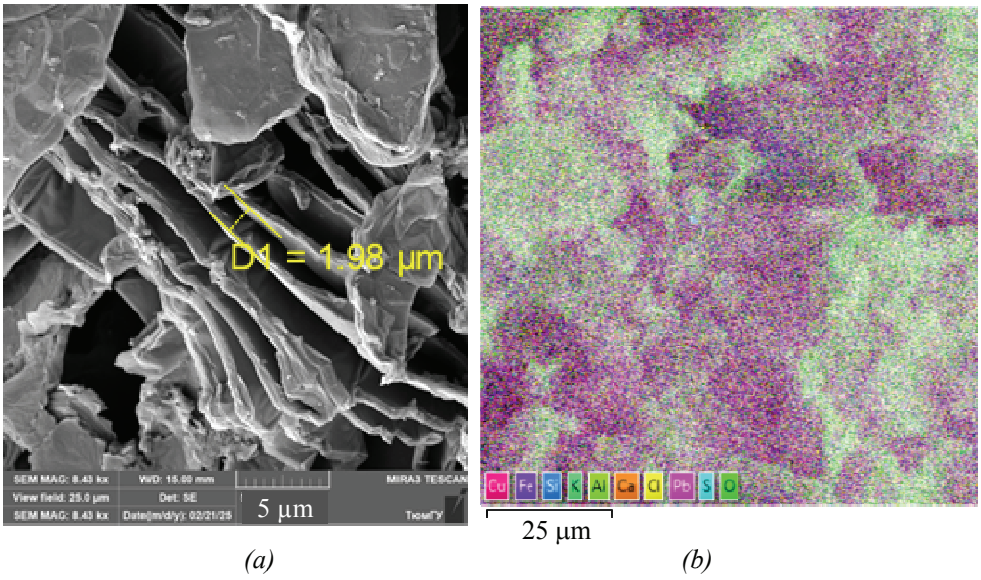

(a) *(b)*

Fig. 8. Carbon material Syn-UO-GO-2.0 after lead sorption:
a – SEM-image of the material surface; *b* – multilayer EDS-image of the sample surface

The fractal dimension of the sample is $D = 2.5957$. In the multilayer EDS-image (Fig. 7*b*), one can observe a non-uniform distribution of various atoms (mainly oxygen and sulfur). The total weight of oxygen atoms is 81.6 %, sulfur – 11.5 % (Fig. S7).

The surface of the Syn-UO-GO-2.0 material after sorption did not change significantly and still has exfoliated graphite sheets, 5–10 µm in size and exfoliations of about ~2 µm (Fig. 8*a*). The fractal dimension after sorption did not change significantly and is: $D = 2.5817$. In the multilayer EDS-image (Fig. 8*b*), one can observe a non-uniform distribution of lead atoms, the total weight of which is 25.0 % (Fig. S8).

3.2. Experimental data on sorption kinetics and their analysis

Figure 9 shows that the moment of equilibrium (plateau on the graphs) for the Nat-OO-GO-4.5 and Syn-OO-GO-4.5 samples occurs after 5 minutes, and for the Syn-UO-GO-2.0 and Syn-UO-GO-1.0 samples – after 30 min from the start of the sorption process. The following values of the maximum sorption capacity Q_e^{exp} were obtained: 105 mg·g^{-1} for Syn-UO-GO-2.0, 108 mg·g^{-1} for Syn-UO-GO-1.0, 130 mg·g^{-1} for Nat-OO-GO-4.5 and 138 mg·g^{-1} for Syn-OO-GO-4.5. The values obtained in this study

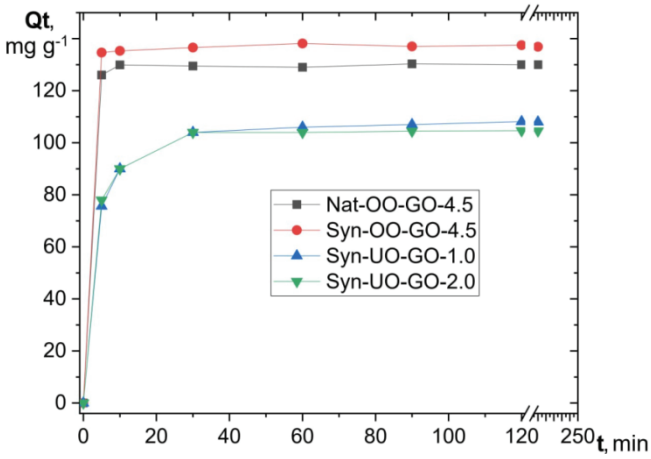

Fig. 9. Dependences of the sorption capacity of samples on time

slightly surpass those reported by other researchers for similar materials in the purification of aqueous media from Pb^{2+}. Furthermore, the equilibrium for Pb^{2+} sorption is reached in the same timeframe or even more rapidly, as illustrated in Table 1.

The higher capacitive and kinetic characteristics of the graphene oxide samples discussed in this article, compared to the materials in Table 1, are justified by the presence of negatively charged surface functional groups and the occurrence of physical sorption in the interlayer space of the pseudocrosslinked structure of the material (for under-oxidized samples), as well as by the high content of functional groups on the surface of the sample (for over-oxidized samples). In this regard, the structure and properties of graphene oxides can be regulated by altering the oxidation state of their surface [15].

Thus, the rate of reaching equilibrium and the maximum value of Q_e^{exp}, are affected by the oxidation state and the nature of graphene oxide. An increase in the oxidation state of graphene oxide (i.e., an increase in the amount of potassium permanganate) leads to an increase in the number of functional groups (sorption centers) on its surface. In addition, synthetic graphene oxide provides a slightly higher sorption capacity than natural graphene oxide.

Similar behavior of these materials was also characteristic in the case of sorption of an organic compound – methylene blue – from aqueous solutions [15].

The experimental data were analyzed using the empirical kinetic and diffusion models from Table 1, and the results of the analysis are presented in Table 2.

As can be seen from the data in the tables, for all samples the experimental data are described by the pseudo-second-order kinetic equation (Ho-McKay), with the correlation coefficient R^2 equal to 1.00. This is also confirmed by the fact that the value of the Q_e parameter of this model almost coincides with the value of the sorption capacity obtained experimentally Q_e^{exp}. The model assumes that the process is limited by the chemical interaction between the sorbent and the sorbate and depends on the concentration of the sorbate and the temperature [36]. The pseudo-first-order kinetic equation (Lagergren), on the contrary, poorly describes the processes occurring on the studied graphene oxide samples, which is confirmed by the low values of the correlation coefficient for all cases.

Table 1. Comparison of different sorbents for Pb^{2+} removal

Sorbent	Q_e, mg·g^{-1}	Phase contact time, min	Reference
Water-soluble magnetic composite based on chitosan and graphene oxide	77	10	[31]
Thiol-functionalized graphene oxide	15–25	50	[32]
Surface polymer with ionic imprinting of Pb(II) based on sandwich graphene oxide composite materials	23	30	[33]
Graphene oxide and carboxylated graphene oxide	37–90	30	[34]
Complex of graphene oxide and chitosan	30–60	70–90	[35]
Graphene oxide natural/synthetic overoxidized/underoxidized	105–138	30; 5	Present paper

Table 2. Parameters of kinetic models for the process of Pb^{2+} sorption on different samples

Sample						
Syn-UO-GO-1.0						
Experiment	Boyd model			Morris-Weber model		
$Q_e^{(exp)} \approx 108$ mg·g^{-1}	R^2			k_{id}	C	R^2
	0.9924			8.2254	60.07	0.9391
	0.9972			0.6557	100.88	0.9937
	Pseudo-first-order model			Pseudo-second-order model		
	k_1	Q_e	R^2	k_2	Q_e	R^2
	–0.0293	8.8369	0.4158	0.0052	108.70	1,00
	Elovich model					
	β		α		R^2	
	0.1219		35023.2		0.8420	
Syn-UO-GO-2.0						
Experiment	Boyd model			Morris-Weber model		
$Q_e^{(exp)} \approx 105$ mg·g^{-1}	R^2			k_{id}	C	R^2
	0.9985			7.6535	62.91	0.9608
	0.7999			0.0677	103.64	0.6806
	Pseudo-first-order model			Pseudo-second-order model		
	k_1	Q_e	R^2	k_2	Q_e	R^2
	–0.0281	5.9088	0.06368	0.008762	105.26	1.00
	Elovich model					
	β		α		R^2	
	0.1566		655353.9		0.7692	
Syn-OO-GO-4.5						
Experiment	Boyd model			Morris-Weber model		
$Q_e^{(exp)} \approx 138$ mg·g^{-1}	R^2			k_{id}	C	R^2
	0.9962			0.5747	133.43	0.9968
	0.00001			0.00021	137.11	0.0004
	Pseudo-first-order model			Pseudo-second-order model		
	k_1	Q_e	R^2	k_2	Q_e	R^2
	–0.0012	0.7071	0.0015	–0.2664	136.99	1.00
	Elovich model					
	β		α		R^2	
	1.4449		2.16^{83}		0.6739	
Nat-OO-GO-4.5						
Experiment	Boyd model			Morris-Weber model		
$Q_e^{(exp)} \approx 130$ mg·g^{-1}	R^2			k_{id}	C	R^2
	0.9336			–0.1978	130.59	0.9994
	0.4286			–0.0377	130.55	0.4748
	Pseudo-first-order model			Pseudo-second-order model		
	k_1	Q_e	R^2	k_2	Q_e	R^2
	–0.0083	1.4873	0.0966	0.0593	129.87	1.00
	Elovich model					
	β		α		R^2	
	1.3385		7.66^{72}		0.4873	

The Elovich equation ($R^2 \approx 0.49–0.84$) is used to describe the sorption process on an energetically heterogeneous surface, and sorption and the reverse process, desorption, affect the kinetics of sorbate (Pb^{2+}) absorption. According to the analysis results (Table 2), one can see that the initial sorption rate α is many times higher than the desorption rate β, which is possibly due to the high availability of active centers on the surface of the studied samples in relation to the amount of sorbate in the solution [37].

In order to explain the sorption behavior of Pb^{2+} on graphene oxide samples, it is necessary to understand the sorption mechanism, taking into account the diffusion processes occurring in the systems under consideration. For this purpose, the models of internal (Morris-Weber) and external (Boyd) diffusion were used in this work (Table 2, Figs. S10–S13).

The kinetic data illustrated in Figs. S10*a*–S13*a* reveal a linear relationship consistent with the Morris-Weber internal diffusion model, which is characterized by two distinct time segments. The initial segment corresponds to bulk diffusion, where Pb^{2+} cations migrate through the solution to reach the outer surface of the sample, leading to rapid sorption. The subsequent segment represents the equilibrium phase. Notably, the presence of a non-zero value of C (as shown in Table 2) suggests that multiple processes, such as film diffusion within the boundary layer, may have influenced the sorption kinetics [37].

The Boyd external diffusion model (Figs. S10*b*–S13*b*) can be used to determine the sorption-limiting stage of external diffusion mass transfer. This model assumes that if the straight line passes through the origin, then the rate-limiting stage is intraparticle diffusion, and if the line does not pass through the origin, then either film diffusion or both film and intraparticle diffusion can control the sorption process [37]. In this case, all figures show that the straight line does not pass through the origin, which suggests that the Pb^{2+} sorption process on graphene oxide samples is presumably controlled by film and intraparticle diffusion processes.

4. Conclusion

During the study, the adsorption properties (in the process of removing lead ions) of four graphene oxide samples, oxidized with varying amounts of potassium permanganate, were investigated, and the surface of the material was analyzed. For all samples, the experimental kinetic data of sorption were approximated using the pseudo-second-order equation. The analysis of internal and external diffusion models indicated that the sorption of Pb^{2+} ions presumably occurs in a mixed-diffusion mode. It was established that with an increase in the oxidation degree of graphene oxide (the amount of oxidizer $KMnO_4$ added during the synthesis), the maximum sorption capacity of the sample increases and the time to reach equilibrium decreases (from 30 to 5 min); specifically, 105 $mg \cdot g^{-1}$ for Syn-UO-GO-2.0, 108 $mg \cdot g^{-1}$ for Syn-UO-GO-1.0, 130 $mg \cdot g^{-1}$ for Nat-OO-GO-4.5, and 138 $mg \cdot g^{-1}$ for Syn-OO-GO-4.5, which exceeded the corresponding values obtained by other researchers for similar materials. The results of the adsorption studies are supported by morphological and elemental composition analysis of their surfaces using SEM and EDS methods. Peaks and valleys with a characteristic “wrinkled” fractal geometry of graphene were found on the surface of the materials, where the sorption of Pb^{2+} ions occurs, and the size of these peaks and valleys depends on the oxidation degree of the graphene oxide surface. Thus, it can be concluded that the structure and sorption properties of graphene oxide can be regulated by varying the oxidation degree as well as the source of graphite (synthetic or natural), which will facilitate new developments in the application of graphene oxide-based materials for the sorptive removal of heavy metals from contaminated water environments.

5. Supplementary Material

https://disk.yandex.ru/i/K6TOUa0c80AslQ

6. Acknowledgements

This research was supported by the Russian Science Foundation, Project Grant No. 25-23-00318, https://rscf.ru/project/25-23-00318/

The authors express their gratitude to A.N. Bobylev, Head of the Memristor Materials Laboratory, Center for Nature-Inspired Engineering (University of Tyumen) for his assistance in conducting the materials study using the SEM and EDS methods.

Besides, this study was partially performed using resources of the Research Resource Center “Natural Resource Management and Physico-Chemical Research” (University of Tyumen).

7. Conflict of interest

The authors declare no conflict of interest.

References

1. Chichigina YaM, Shigabaeva GN, Emelyanova EA, Galunin EV, et al. Heavy metal contents in the Tyumen city residential area soils. *Journal of Advanced Materials and Technologies*. 2023;8(2):141-156. DOI:10.17277/jamt.2023.02
2. Kumar V, Dwivedi SK, Oh S. A critical review on lead removal from industrial wastewater: recent advances and future outlook. *Journal of Water Process Engineering*. 2022;45:102518. DOI:10.1016/j.jwpe.2021.102518
3. Binh NTL, Hoang NT, Truc NTT, Khang VD, |et al. Estimating the possibility of lead contamination in soil surface due to lead deposition in atmosphere. *Journal of Nanomaterials*. 2021;2021:1-7. DOI:10.1155/2021/5586951
4. Burakov AE, Galunin EV, Burakova IV, Kucherova AE, et al. Adsorption of heavy metals on conventional and nanostructured materials for wastewater treatment purposes: a review. *Ecotoxicology and Environmental Safety*. 2018;148:702-712. DOI:10.1016/j.ecoenv.2017.11.034
5. Kaźmierczak J, Nowicki P, Pietrzak R. Sorption properties of activated carbons obtained from corn cobs by chemical and physical activation. *Adsorption*. 2013;19(2-4):273-281. DOI:10.1007/s10450-012-9450-y
6. Nowicki P, Kazmierczak J, Pietrzak R. Comparison of physicochemical and sorption properties of activated carbons prepared by physical and chemical activation of cherry stones. *Powder Technology*. 2015;269:312-319. DOI:10.1016/j.powtec.2014.09.023
7. Baimenov A, Berillo DA, Poulopoulos SG, Inglezakis VJ. A review of cryogels synthesis, characterization and applications on the removal of heavy metals from aqueous solutions. *Advances in Colloid and Interface Science*. 2020;276:102088. DOI:10.1016/j.cis.2019.102088
8. Lazzari LK, Zampieri VB, Neves RM, Zanini M, et al. A study on adsorption isotherm and kinetics of petroleum by cellulose cryogels. *Cellulose*. 2019;26(2):1231-1246. DOI:10.1007/s10570-018-2111-x
9. Baimenov A, Montagnaro F, Inglezakis VJ, Balsamo M. Experimental and modeling studies of Sr^{2+} and Cs^{+} sorption on cryogels and comparison to commercial adsorbents. *Industrial & Engineering Chemistry Research*. 2022;61(23):8204-8219. DOI:10.1021/acs.iecr.2c00531
10. Najafi M, Yousefi Y, Rafati AA. Synthesis, characterization and adsorption studies of several heavy metal ions on amino-functionalized silica nano hollow sphere and silica gel. *Separation and Purification Technology*. 2012;85:193-205. DOI:10.1016/j.seppur.2011.10.011
11. He S, Zhao C, Yao P, Yang S. Chemical modification of silica gel with multidentate ligands for heavy metals removal. *Desalination and Water Treatment*. 2016;57(4):1722-1732. DOI:10.1080/19443994.2014.977958
12. Da'na E. Adsorption of heavy metals on functionalized-mesoporous silica: a review. *Microporous and Mesoporous Materials*. 2017;247:145157. DOI:10.1016/j.micromeso.2017.03.050
13. Zaidi R, Khan SU, Farooqi IH, Azam A. Investigation of kinetics and adsorption isotherm for fluoride removal from aqueous solutions using mesoporous cerium–aluminum binary oxide nanomaterials. *RSC Advances*. 2021;11(46):28744-28760. DOI:10.1039/D1RA00598G
14. Tabish TA, Memon FA, Gomez DE, Horsell DW, et al. A facile synthesis of porous graphene for efficient water and wastewater treatment. *Scientific Reports*. 2018;8(1):1817. DOI:10.1038/s41598-018-19978-8
15. Ioni Y, Ibragimova V, Sapkov I, Dimiev A. Graphene oxide with different oxygen content produced from natural and synthetic graphite sources for methylene blue sorption. *Diamond and Related Materials*. 2024;149:111550. DOI:10.1016/j.diamond.2024.111550
16. Bulin C, Ma Z, Guo T, Li B, et al. Magnetic graphene oxide nanocomposite: one-pot preparation, adsorption performance and mechanism for aqueous Mn(II) and Zn(II). *Journal of Physics and Chemistry of Solids*. 2021;156:110130. DOI:10.1016/j.jpcs.2021.110130
17. Maged A, Kharbish S, Ismael IS, Bhatnagar A. Characterization of activated bentonite clay mineral and the mechanisms underlying its sorption for ciprofloxacin from aqueous solution. *Environmental Science and Pollution Research*. 2020;27(26):32980-32997. DOI:10.1007/s11356-020-09267-1
18. Wahab N, Saeed M, Ibrahim M, Munir A, et al. Synthesis, characterization, and applications of silk/bentonite clay composite for heavy metal removal from aqueous solution. *Frontiers in Chemistry*. 2019;7:654. DOI:10.3389/fchem.2019.00654
19. Cui L, Guo X, Wei Q, Wang Y, et al. Removal of mercury and methylene blue from aqueous solution by xanthate functionalized magnetic graphene oxide: sorption kinetic and uptake mechanism. *Journal of Colloid and Interface Science*. 2015;439:112-120. DOI:10.1016/j.jcis.2014.10.019
20. *Free encyclopedia Wikipedia. Article "Graphite Oxide"*. Available from: https://ru.wikipedia.org/wiki/Оксид_графита [Accessed 8December 2024]
21. Ioni Y, Khamidullin T, Sapkov I, Brusko V, et al. Revealing the effect of graphite source on the properties of synthesized graphene oxide. *Carbon Letters*. 2024;34(4):1219-1228. DOI:10.1007/s42823-023-00680-3
22. Burakov AE, Burakova IV, Kucherova AE, Blokhin AN. *Adsorption from solutions: structural and functional characteristics of nanomaterials: a textbook*. Tambov: TSTU Publ. house; 2016. p. 49-50. Available from: https://tstu.ru/book/elib1/exe/2016/Burakov.exe (In Russ.)
23. Lagergren SK. About the theory of so-called adsorption of soluble substances. *Sven. Vetenskapsakad. Handingarl*. 1898;24:1-39.

24. Ho YS, McKay G. Sorption of dye from aqueous solution by peat. *Chemical Engineering Journal*. 1998; 70(2):115-124. DOI:10.1016/S0923-0467(98)00076-1

25. Elovich SYu, Larionov OG. Theory of adsorption from nonelectrolyte solutions on solid adsorbents: 1. Simplified analysis of the equation of the adsorption isotherm from solutions. *Bulletin of the Academy of Sciences of the USSR Division of Chemical Science*. 1962;11(2):191-197. DOI:10.1007/BF00908016

26. Weber W, Morris J. Intraparticle diffusion during the sorption of surfactants onto activated carbon. *Journal of the Sanitary Engineering Division American Society of Civil Engineers*. 1963;89(1):53-61.

27. Boyd GE, Schubert J, Adamson AW. The exchange adsorption of ions from aqueous solutions by organic zeolites. Ion-exchange equilibria. *Journal of the American Chemical Society*. 1947;69(11):2818-2829. DOI:10.1021/ja01203a064

28. Rathour RKS, Singh H, Bhattacharya J, Mukherjee A. Sand coated with graphene oxide-PVA matrix for aqueous Pb^{2+} adsorption: Insights from optimization and modeling of batch and continuous flow studies. *Surfaces and Interfaces*. 2022;32:102115. DOI:10.1016/j.surfin.2022.102115

29. Liu M, Weston PJ, Hurt RH. Controlling nanochannel orientation and dimensions in graphene-based nanofluidic membranes. *Nature Communications*. 2021;12(1):507. DOI:10.1038/s41467-020-20837-2

30. Liebovitch LS, Toth T. A fast algorithm to determine fractal dimensions by box counting. *Physics Letters A*. 1989;141(8-9):386-390. DOI:10.1016/0375-9601(89)90854-2

31. Fan L, Luo C, Sun M, Li X, et al. Highly selective adsorption of lead ions by water-dispersible magnetic chitosan/graphene oxide composites. *Colloids and Surfaces B: Biointerfaces*. 2013;103:523-529. DOI:10.1016/j.colsurfb.2012.11.006

32. Yari M, Rajabi M, Moradi O, Yari A, et al. Kinetics of the adsorption of Pb(II) ions from aqueous solutions by graphene oxide and thiol functionalized graphene oxide. *Journal of Molecular Liquids*. 2015;209:50-57. DOI:10.1016/j.molliq.2015.05.022

33. Huang R, Shao N, Hou L, Zhu X. Fabrication of an efficient surface ion-imprinted polymer based on sandwich-like graphene oxide composite materials for fast and selective removal of lead ions. *Colloids and Surfaces A: Physicochemical and Engineering Aspects*. 2019;566:218-228. DOI:10.1016/j.colsurfa.2019.01.011

34. Yang W, Cao M. Study on the difference in adsorption performance of graphene oxide and carboxylated graphene oxide for Cu(II), Pb(II) respectively and mechanism analysis. *Diamond and Related Materials*. 2022;129:109332. DOI:10.1016/j.diamond.2022.109332

35. Li L, Zhao L, Ma J, Tian Y. Preparation of graphene oxide/chitosan complex and its adsorption properties for heavy metal ions. *Green Processing and Synthesis*. 2020;9(1):294-303. DOI:10.1515/gps-2020-0030

36. Slepchenko MA, Slepchenko DA, Paul′ ES. Kinetic models of sorption. *Nauchnyylider*. 2025;7(208):147-150. (In Russ.)

37. Kuznetsova TS, Burakov AE, Ananyeva OA, Burakova IV, et al. Kinetics of lead sorption from aqueous solutions on nanostructured cryogel modified with organic polymers. *Colloid Journal*. 2024;86(3):408-417. DOI:10.1134/S1061933X24600131

Information about the authors / Информация об авторах

Ilya V. Tulupov, Student, University of Tyumen (UTMN), Tyumen, Russian Federation; ORCID 0009-0004-8585-8862; e-mail: stud0000273398@study.utmn.ru

Тулупов Илья Вадимович, студент, Тюменский государственный университет (ТюмГУ), Тюмень, Российская Федерация; ORCID 0009-0004-8585-8862; e-mail: stud0000273398@study.utmn.ru

Lyubov E. Sosnovskikh, Student, UTMN, Tyumen, Russian Federation; ORCID 0009-0004-0125-1829; e-mail: stud0000263318@study.utmn.ru

Сосновских Любовь Евгеньевна, студент, ТюмГУ, Тюмень, Российская Федерация; ORCID 0009-0004-0125-1829; e-mail: stud0000263318@study.utmn.ru

Viktoriya R. Ibragimova, Senior Research Lab Assistant, Kurnakov Institute of General and Inorganic Chemistry of the Russian Academy of Sciences (IGIC RAS), Moscow, Russian Federation; Student, Lomonosov Moscow State University, Moscow, Russian Federation; ORCID 0000-0001-7222-7771; e-mail: vika.ibragimova.2002@bk.ru

Ибрагимова Виктория Руслановна, старший лаборант-исследователь, Институт общей и неорганической химии им. Н. С. Курнакова РАН (ИОНХ РАН), Москва, Российская Федерация; студент, Московский государственный университет имени М. В. Ломоносова, Москва, Российская Федерация; ORCID 0000-0001-7222-7771; e-mail: vika.ibragimova.2002@bk.ru

Yuliya V. Ioni, Cand. Sc. (Chem.), Research Assistant, IGIC RAS, Moscow, Russian Federation; ORCID 0000-0001-5108-4329; e-mail: acidladj@mail.ru

Иони Юлия Владимировна, кандидат химических наук, научный сотрудник, ИОНХ РАН, Москва, Российская Федерация; ORCID 0000-0001-5108-4329; e-mail: acidladj@mail.ru

Aleksei Yu. Isaev, Senior Lecturer, UTMN, Tyumen, Russian Federation; ORCID 0000-0002-2163-9968; e-mail: a.yu.isaev@utmn.ru

Evgeny V. Galunin, Ph.D. in Analytical Chemistry, Professor, UTMN, Tyumen, Russian Federation; ORCID 0000-0002-8219-0148; e-mail: e.v.galunin@utmn.ru

Farid K. Shabiev, Cand. Sc. (Phys.-Math.), Professor, UTMN, Associate Professor, Industrial University of Tyumen, Tyumen, Russian Federation; ORCID 0000-0003-0551-3836; e-mail: f.k.shabiev@utmn.ru

Gulnara N. Shigabaeva, Cand. Sc. (Eng.), Professor, Head of the Department, UTMN, Tyumen, Russian Federation; ORCID 0000-0003-2116-1017; e-mail: g.n.shigabaeva@utmn.ru

Исаев Алексей Юрьевич, старший преподаватель, ТюмГУ, Тюмень, Российская Федерация; ORCID 0000-0002-2163-9968; e-mail: a.yu.isaev@utmn.ru

Галунин Евгений Валерьевич, Ph.D. по аналитической химии, профессор, ТюмГУ, Тюмень, Российская Федерация; ORCID 0000-0002-8219-0148; e-mail: e.v.galunin@utmn.ru

Шабиев Фарид Канафеович, кандидат физико-математических наук, профессор, ТюмГУ, доцент, Тюменский индустриальный университет, Тюмень, Российская Федерация; ORCID 00000-0003-0551-3836; e-mail: f.k.shabiev@utmn.ru

Шигабаева Гульнара Нургаллаевна, кандидат технических наук, профессор, заведующий кафедрой, ТюмГУ, Тюмень, Российская Федерация; ORCID 0000-0003-2116-1017; e-mail: g.n.shigabaeva@utmn.ru

Received 05 May 2025; Revised 26 June 2025; Accepted 30 June 2025